

# PEP-N Simulation and Multihadron Detection

M. Negrini  
*Università di Ferrara – INFN*  
 M. Posocco  
*Università di Padova – INFN*

In this paper we present some results for the simulation of multihadron events in the PEP-N detector. Energies and angular distribution for single particles are presented. Then the detection efficiencies for single particles and for reconstruction of some processes are given.

## 1. THE PEP-N DETECTOR

The PEP-N experiment is proposed to study  $e^+e^-$  collisions occurring between the LER (SLAC Low Energy Ring) positrons, which have a fixed energy of 3.12 GeV, and the electrons stored in the VLER (Very Low Energy Ring) with energy variable in the range 0.2 GeV to 0.8 GeV, which correspond to center of mass energies from about 1.5 GeV to 3.1 GeV. Because of this, the  $e^+e^-$  center of mass (CM) system has a boost in the  $e^+$  beam direction (forward direction). The PEP-N detector (Figure 1) has been designed to fit into a dipole vertical magnet and to have the highest possible acceptance for the reconstruction of the exclusive final states. Because of the boost of the final state particles the detector is not symmetric: the interaction point (IP) is located 25 cm upstream with respect to the center of the magnet, to take advantage of a longer path for the charged particles into the magnetic field.

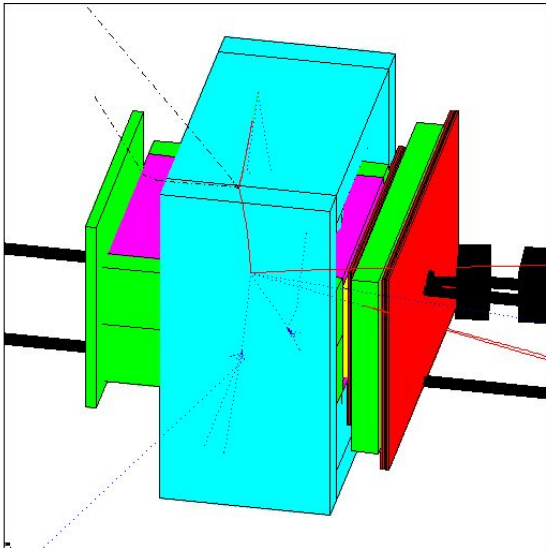


Figure 1: 3D view of PEP-N detector. The dipole magnet surrounds the detector system. LER and VLER pipes are shown with their dipole and quadrupole magnets. A  $\pi^+\pi^-2\pi^0$  reaction is simulated.

### 1.1. Magnet

The simulated magnet is a vertical dipole magnet. The distance between the poles is 120 cm and the distance between the vertical yokes is 240 cm; this is the space into which the detector has to fit (see Figure 2). The pole diameter is 120 cm and the field intensity is about 0.3 T.

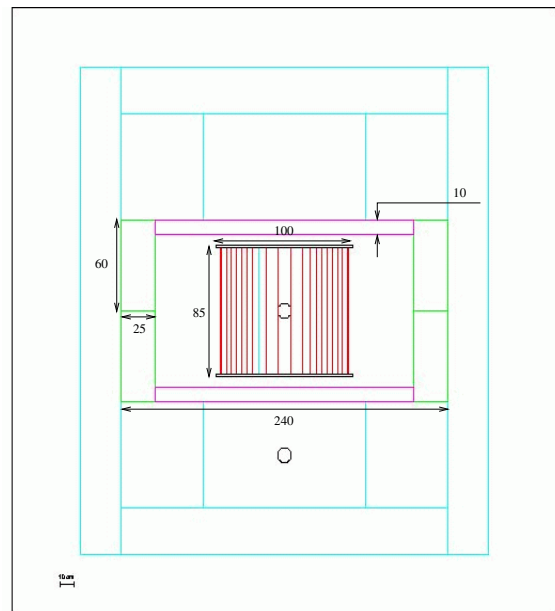


Figure 2: Front section of PEP-N detector. The dipole magnet surrounds all of the detector. The TPC is centered between the poles and the calorimeter system (BCAL + PCAL) gives complete azimuthal coverage.

### 1.2. TPC

The TPC is box-shaped with dimensions 100 cm · 100 cm · 85 cm. It is positioned in the center of the magnet poles (region where the magnetic field is more homogeneous). Since the

interaction point is located 25 cm upstream with respect to the center of the magnet, the pad geometry is not symmetrical for forward and backward tracks. In the simulation, a pad length of 3 cm has been assumed; this results in a number of pad layers varying from 24 (for particles going in the forward direction) to 8 (for particles moving backward). The top view of the TPC in the detector layout is shown in Figure 3.

The momentum resolution of the TPC has been estimated under the hypothesis of  $200 \mu\text{m}$  spatial resolution, assumed to be constant for all track directions. It varies with the particle momentum as well as with the number of hit pad layers. Some results are collected in Table I.

Table I  $\Delta p/p$  for the TPC as a function of the number of hit pad layers and particle momentum. Multiple scattering is not included: it contributes for an additional  $\sim 1\%$  (for He gas).

Transv. p (GeV)	22 points ( <i>forward track</i> )	22 points + 1 point at 120 cm	14 points	6 points ( <i>backward track</i> )
0.1			1.0%	9%
0.2	0.7%	0.3%	2.0%	17%
0.4	1.4%	0.7%	4.1%	
0.6	2.0%	1.0%	6.1%	
0.8	2.7%	1.4%	8.1%	
1.0	3.3%	1.7%		
1.2	4.0%	2.1%		
1.4	4.6%	2.4%		
1.6	5.3%	2.8%		

### 1.3. Calorimeter system

The proposed calorimeters are sandwiches of scintillating fiber layers (1 mm) and lead planes (1 mm), similar to the ones used by KLOE [1]. Two kinds of calorimeters have been simulated, with thickness varying according to the available space:

- **Forward (FCAL) and Barrel (BCAL) calorimeters** have a thickness of 25 cm (corresponding to about 15 radiation lengths). The efficiency is about 99% for photon energy above 20 MeV. The energy resolution is  $\sigma(E)/E \simeq 5\%/\sqrt{E}$ ;
- **Pole (PCAL) and Rear (RCAL) calorimeters** have a thickness of 10 cm, which is the available space between the TPC plates and the magnet poles. The efficiency for such a calorimeter is above 95% for photon energy above 20 MeV and  $\sim 98\%$  for  $E > 40$  MeV. The energy resolution is assumed to be  $\sigma(E)/E \simeq 23\%$  (constant with E).

FCAL has a rectangular hole of  $88 \text{ cm} \cdot 60 \text{ cm}$  corresponding to the LER and VLER beam pipes and focusing and bending

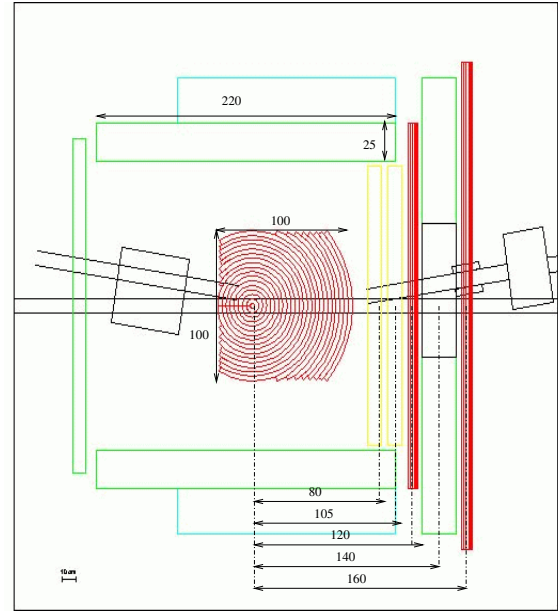


Figure 3: Top section of PEP-N detector. The dipole magnet surrounds all of the detector. The TPC is centered between the poles. In the forward direction two aerogel detectors are present, one tracking chamber, FCAL and an additional tracking chamber. The LER and VLER pipes with magnets are also shown.

magnets; it is positioned between 125 cm and 150 cm from the IP in the forward direction (Figure 3). BCAL modules are located next to magnet yokes and PCAL modules are adjacent to the magnet poles (Figure 2). RCAL is located in the backward direction.

The hadron calorimeter has not been included into the simulation.

### 1.4. Aerogel

The separation between  $K^\pm$  and  $\pi^\pm$  in the momentum range from 0.6 GeV to 1.5 GeV is performed with the aerogel detector. Two layers of the aerogel detector are simulated in the forward direction at a distance of 80 cm and 95 cm respectively from the interaction point. Each one of them has a 5% probability of misidentification of  $K^\pm$  and 0.05% probability of misidentification of  $\pi^\pm$  [2]. For lower momentum particles, the separation could be performed looking at  $dE/dx$  in the TPC or time-of-flight, so no aerogel detector is inserted in side and backward direction, where a small fraction of charged particles have a momentum reaching 0.6 GeV. As an example, in the case of  $2\pi^+2\pi^-2\pi^0$  at 2.0 GeV, about 85% of the  $\pi^\pm$  with momentum between 0.6 GeV and 1.5 GeV have  $\theta < 35^\circ$  (forward direction).

### 1.5. Forward tracking system

Two additional tracking chambers are inserted between the aerogel and the forward calorimeter (120 cm from the IP) and

after the forward calorimeter (160 cm from the IP). These can be used to improve tracking resolution (Table I) as well as to increase acceptance for charged particles at small angles.

## 2. FEATURES OF MULTIHADRON CHANNELS

A first evaluation of PEP-N detector acceptance can be obtained applying a Lorentz boost to a uniform distribution of charged particles and looking at the number of particles that are lost into the beam pipe. From Figure 4 it can be noted that the geometric acceptance for a 100 mrad cut in the forward direction (which corresponds to the dimension of the beam pipe at the far end of the TPC) is  $\sim 98\%$ .

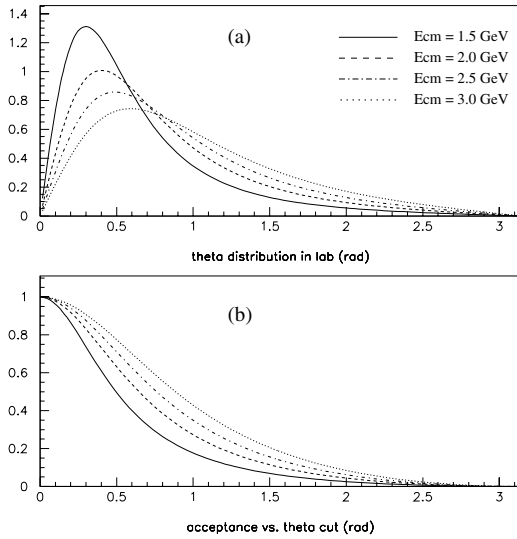


Figure 4: Single particle  $\theta$  distribution (a) and particle acceptance as a function of the polar angle cut (b) for some values of the energy in CM. Cutting at 100 mrad the acceptance turns out to be about 98%.

### 2.1. Charged particles

Figure 5 shows a typical momentum distribution for  $\pi^\pm$ . The high momentum particles are located mostly in the forward direction. More than 70% of the charged tracks hit 20 or more TPC pad layers: this leads to a  $\Delta p/p$  between 1% and 5% (from Table I). Particles moving close to the vertical direction hit few TPC layers so their momentum cannot be measured. In any case the fraction of particles being emitted at small angle with respect to the vertical is very small: as an example, for  $4\pi$  channel at 2.0 GeV, 0.5% of pions have a direction within  $\pm 10^\circ$  from the vertical, 1.4% within  $\pm 15^\circ$  and 2.4% within  $\pm 20^\circ$ .

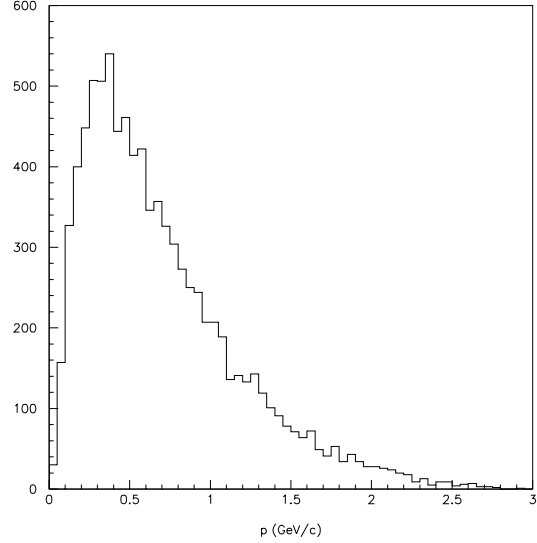


Figure 5: Momentum distribution of charged pions from  $2\pi^+2\pi^-2\pi^0$  reaction at 2.0 GeV CM energy.

Table II Fraction of photons going into each calorimeter for different values of CM energy.

CM Energy	FCAL	BCAL	PCAL	RCAL	Not detected
1.5 GeV	42.2%	9.3%	30.5%	0.5%	17.5%
2.0 GeV	35.4%	13.6%	37.9%	0.5%	12.6%
2.5 GeV	31.2%	14.1%	44.5%	0.8%	9.4%
3.0 GeV	25.8%	17.8%	47.4%	1.2%	7.8%

### 2.2. Photons from $\pi^0$ decay

Figure 6 shows a typical energy distribution for photons coming from a  $\pi^0$  decay. The peak of the distribution is at very low energy (below 300 MeV), moreover the high energy photons (above 1 GeV) are located in the forward direction at  $\theta < 60^\circ$ . The distribution of photons in the various kinds of calorimeter varies with the energy. The results are summarized in Table II.

Moving BCAL modules closer to the IP the acceptance of BCAL can be increased and, at the same time, the acceptance of PCAL will decrease.

## 3. DETECTOR ACCEPTANCE FOR MULTIHADRON

Table III gives the proportions between several multihadron final states. In all of the following, the Monte Carlo events for R acceptance studies are simulated according to this table.

The first step is to analyze the acceptances for the various channels exclusive final states. The hypothesis here is that the final state could be completely determined even if one particle is lost. In what follows a particle is considered to be detected if:

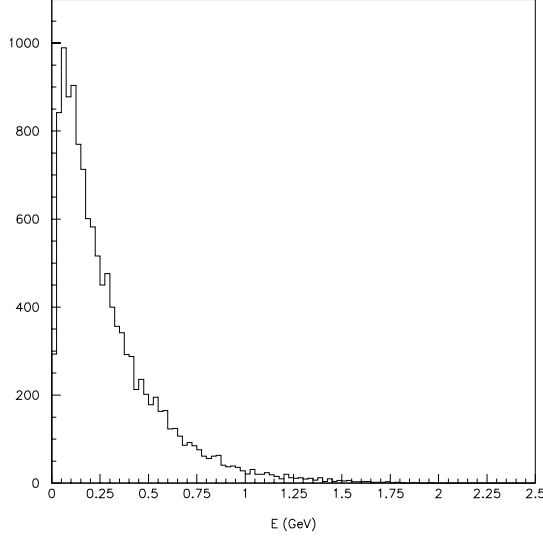


Figure 6: Energy distribution of photons coming from  $\pi^0$  decay from  $2\pi^+2\pi^-2\pi^0$  reaction at 2.0 GeV CM energy.

- $\pi^\pm$  or  $K^\pm$ : 5 or more TPC pad layers hit. Identification of  $\pi$  and  $K$  for  $p < 1.5$  GeV is assumed to be done with  $dE/dx$  or time of flight (TOF) (small  $p$ ) or aerogel (high  $p$ );
- $\gamma$ : cut at 20 MeV and calorimeter efficiency applied.

Under these assumptions, two photons are requested to have the  $\pi^0$  invariant mass, with a  $3\sigma$  cut (see Figure 7), to tag the  $\pi^0$  itself.

The capability of PEP-N detector to detect hadron resonances has been studied producing  $\omega\pi^0$  (50%) and  $\pi^+\pi^-2\pi^0$  (50%). The reconstructed  $\omega$  peak (Figure 8) has a width of  $\sim 30$  MeV.

#### 4. EFFICIENCY FOR R MEASUREMENT

For a precision measurement of  $R$ , it is very important to be able to determine with good accuracy the cross sections of exclusive final states in order to get a small systematic error related to acceptances uncertainty. In the following we summarize the results for the acceptance on  $R$  measurement simulation performed with both exclusive and inclusive methods [3]. No background or channel misidentification are taken into account in this study. All channels are simulated using phase space distribution.

##### 4.1. Exclusive method

Each channel should be measured and identified. Table IV gives the detection efficiency in the two cases in which all particles are detected or one particle is lost. For the detection

Table III Proportions between multihadrons final states at 1.5 GeV and 2.0 GeV.

Final state	1.5 GeV	2.0 GeV
$\pi^+\pi^-$	3%	-
$\pi^+\pi^-\pi^0$	4%	1.5%
$\pi^+\pi^-2\pi^0$	40%	21.5%
$2\pi^+2\pi^-$	36%	16%
$2\pi^+2\pi^-\pi^0$	2%	1%
$\pi^+\pi^-3\pi^0$	1%	0.5%
$2\pi^+2\pi^-2\pi^0$	6%	24%
$3\pi^+3\pi^-$	1%	5%
$\pi^+\pi^-4\pi^0$	2%	8%
$K^+K^-$	4%	1.5%
$K^+K^-\pi^0$	1%	3%
$K^+K^-\pi^+\pi^-$	-	8%
$K^+K^-2\pi^0$	-	4%
$K_S K_L$	-	0.5%
$K_S K_L \pi^+\pi^-$	-	4%
$K_S K_L 2\pi^0$	-	1.5%

Table IV Detection efficiency for some multihadron final states when all particles of the final state are detected and when only one particle is lost. For final states in which a  $K^\pm$  is present, at least one of them is required to be identified as kaon. The results are obtained for a CM energy of 2 GeV. The overall detection efficiency for the considered channels (obtained weighing with the various final states relative cross sections in table III) in the case of at most one lost particle is  $\sim 88\%$ .

Final state	All detected	1 lost
$\pi^+\pi^-\pi^0$	76.5%	98.8%
$\pi^+\pi^-2\pi^0$	56.3%	94.1%
$2\pi^+2\pi^-$	89.4%	99.8%
$2\pi^+2\pi^-\pi^0$	68.5%	97.9%
$\pi^+\pi^-3\pi^0$	44.3%	86.9%
$2\pi^+2\pi^-2\pi^0$	52.0%	82.8%
$3\pi^+3\pi^-$	82.5%	99.1%
$\pi^+\pi^-4\pi^0$	30.2%	72.0%
$K^+K^-$	29.6%	29.7%
$K^+K^-\pi^0$	54.1%	72.3%
$K^+K^-\pi^+\pi^-$	82.0%	90.9%
$K^+K^-2\pi^0$	54.1%	85.9%

of channels with  $K^\pm$ , at least one of the two is required to be identified by  $dE/dx$ , TOF or aerogel.

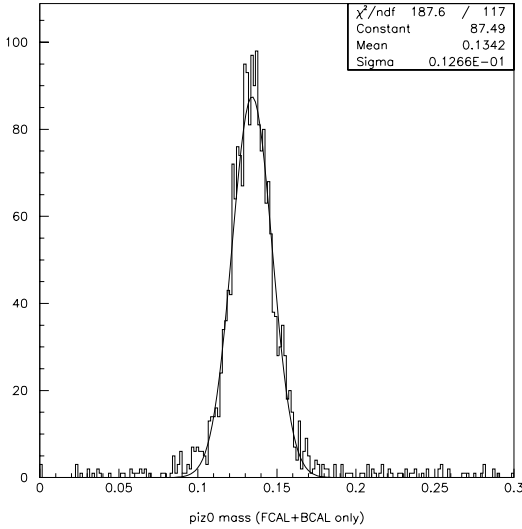


Figure 7:  $\pi^0$  reconstructed invariant mass. In this case both photons are detected in FCAL or BCAL. If both  $\gamma$  are detected in PCAL the width increases to  $\sim 0.02$  GeV.

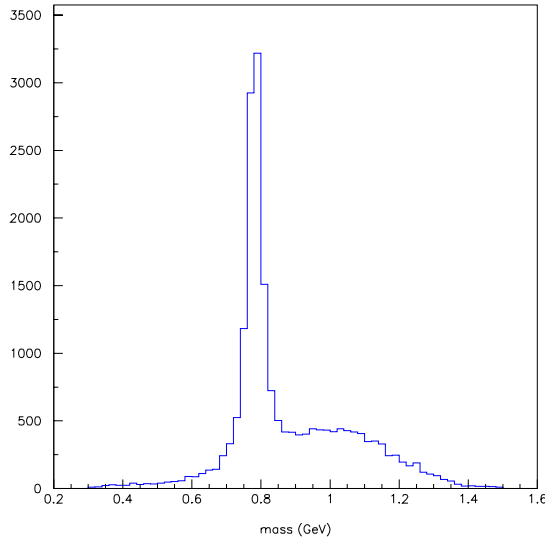


Figure 8:  $\omega$  reconstructed mass for  $\omega\pi^0$  events on  $\pi^+\pi^-2\pi^0$  background.

## 4.2. Inclusive method

In principle, the R measurement could be done by requiring that at least one hadron be observed in the final state. Of course this method leads to a greater systematic uncertainty when evaluating the cross section of such a process related to the difficulty of measuring the overall acceptance. Anyway this is still a possibility that has to be considered, so an evaluation of PEP-N detection efficiency for this kind of measurement has been done. Since up to now the background is not known, instead of requiring one hadron detected in the final state, an event was accepted if it satisfied at least one of the following cuts:

- $n_{\pi^\pm} \geq 3$
- $n_{\pi^\pm} \geq 2$  and  $n_\gamma \geq 1$
- $n_{\pi^\pm} \geq 1$  and  $n_{\pi^0} \geq 1$
- $n_{K^\pm} \geq 1$
- $n_{\pi^\pm} \geq 1$  and  $n_{K_S} \geq 1$

in this case the  $K_S$  is assumed to be detected if there are high energy depositions in calorimeter from  $K_S$  decay.

The overall detection efficiency is 95.6% at 1.5 GeV CM energy and 96.3% at 2.0 GeV. Inefficiencies are mostly due to  $\pi^+\pi^-$  at low CM energy (always rejected from the former cuts) and  $K_S K_L X$  at high energy. A more detailed analysis will probably recover part of these inefficiencies.

## REFERENCES

- [1] KLOE Collaboration, "Calibration and reconstruction performances of the KLOE e.m. calorimeter," to be published on Proc. IX Intl. Conference on Calorimetry in Part. Phys. Anney, Oct 9–14 2000
- [2] A. Yu. Barnyakov et al., "Test of aerogel counters for the KEDR detector," to be published, February 2001.
- [3] D. Bettoni, "Detector layout," published in this proceedings.